# Tunable Mass Separation via Negative Mobility

A. Słapik,[1] J. Łuczka,[1] P. Hänggi,[2,3] and J. Spiechowicz[1,2]
[1]Institute of Physics and Silesian Center for Education and Interdisciplinary Research, University of Silesia, 41-500 Chorzów, Poland
[2]Institute of Physics, University of Augsburg, D-86135 Augsburg, Germany
[3]Nanosystems Initiative Munich, Schellingstraße 4, D-80799 München, Germany

(Received 19 September 2018; revised manuscript received 22 November 2018; published 21 February 2019)

A prerequisite for isolating diseased cells requires a mechanism for effective mass-based separation. This objective, however, is generally rather challenging because typically no valid correlation exists between the size of the particles and their mass value. We consider an inertial Brownian particle moving in a symmetric periodic potential and subjected to an externally applied unbiased harmonic driving in combination with a constant applied bias. In doing so, we identify a most efficient separation scheme which is based on the anomalous transport feature of negative mobility, meaning that the immersed particles move in the direction opposite to the acting bias. This work is the first of its kind in demonstrating a *tunable* separation mechanism in which the particle mass targeted for isolation is effectively controlled over a regime of nearly 2 orders of mass magnitude upon changing solely the frequency of the external harmonic driving. This approach may provide mass selectivity required in present and future separation of a diversity of nano- and microsized particles of either biological or synthetic origin.

DOI: 10.1103/PhysRevLett.122.070602

The objective of separating and sorting particles of small size is attracting growing interest [1–20], opening the way towards the precise analysis of biophysical and synthetic processes on the microscale. In this regime of sizes the omnipresent Brownian jitter dynamics is of relevant impact. Nowadays, effective isolation and separation techniques are of essential importance in a wide range of areas including both research and industrial applications. Particularly, such techniques carry a large potential to study selective transport of biological particles such as whole cells, organelles, or DNA complexes. It has been found that several diseases alter physical properties of cells and therefore their sorting has great significance in health care [21]. So far, much emphasis has been placed on size based isolation techniques [6,7,10–13,15–18,20]. However, another aspect representing one of the most important factors for specifically identifying a bioparticle presents its own mass. For instance, cancer cells are found to differ in mass as compared to healthy ones [21]. This fact suggests that mass heterogeneity might be an important factor associated with disease initiation and progression. A reliable and effective approach to separating particles by their masses is therefore much in demand and hence one needs to learn more about various mechanisms for separating different masses on the Brownian scale [14,22,23]. As is commonly appreciated, the task is challenging because of the fact that heavier objects do not necessarily imply also larger sizes. This very feature thereby excludes passive mechanical separation techniques such as filtration in artificial sieves [24].

In the following, we demonstrate a nonintuitive, yet efficient, mass-based separation strategy taking advantage of a paradoxical mechanism of negative mobility (NM) [3,25–29]. In a regime of NM the particles move in a direction opposite to the net acting force. This phenomenon rests on two main ingredients: (i) a spatially periodic nonlinear structure together with (ii) an inertial nonequilibrium stochastic dynamics created, for example, via a time-periodic varying driving force of vanishing mean value. We demonstrate that under an additional action of an applied constant bias only particles of a given mass migrate in the direction opposite to this net force, whereas the others move concurrently towards it. This opens the possibility of steering different particle species in opposite directions under identical experimental conditions. Moreover, we demonstrate that the mass targeted for separation can be tuned by nearly 2 orders of magnitude by changing only the frequency of external time-periodic driving. The proof of principle experiment of a similar separation scheme but based rather on the particle size has been already demonstrated in Refs. [30,31], using a lab-on-a-chip device, consisting of insulator dielectrophoresis in a nonlinear, symmetric microfluidic structure with electrokinetically induced transport. This system was built employing a photolithographic device fabrication strategy without the need of making use of more complex nanofabrication techniques. Very recently, it allowed one to induce not only for colloidal particles but even for a biological compound in the form of mouse liver mitochondrion [32]. Therefore, the separation scheme proposed here

 

may provide mass selectivity required for individual isolation of nano- and microparticles, proteins, organelles, and cells. Yet other suitable setups which allow one to test our theoretical predictions would be based on cold atoms dwelling in optical lattices [33,34].

Let us consider a classical inertial Brownian particle dynamics of mass $M$ moving in a spatially periodic one-dimensional potential $U(x) = U(x + L)$ of period $L$ which is subjected to an unbiased time-periodic force $A\cos(\Omega t)$ of amplitude $A$ and angular frequency $\Omega$, as well as an external static force $F$. The Brownian dynamics of such a particle is described by the Langevin equation [35]

$$M\ddot{x} + \Gamma\dot{x} = -U'(x) + A\cos(\Omega t) + F + \sqrt{2\Gamma k_B T}\xi(t). \quad (1)$$

The parameter $\Gamma$ denotes the friction coefficient and $k_B$ is the Boltzmann constant. The periodic potential $U(x)$ is taken to possess *reflection symmetry* with period $L$ and a potential height $2\Delta U$, i.e.,

$$U(x) = \Delta U \sin\left(\frac{2\pi}{L}x\right). \quad (2)$$

The interaction with a heat bath of temperature $T$ is described by thermal fluctuations modeled by Gaussian white noise of zero mean and unit intensity, i.e.,

$$\langle\xi(t)\rangle = 0, \qquad \langle\xi(t)\xi(s)\rangle = \delta(t - s). \quad (3)$$

Despite the apparent simplicity of this model setup it exhibits peculiar transport behaviors including, e.g., a nonequilibrium noise enhanced transport efficiency [28], anomalous diffusion [36], amplification of normal diffusion [37,38], or also a nonmonotonic temperature dependence of normal diffusion [39].

For our analysis we first recast Eq. (1) into its dimensionless form, i.e.,

$$m\ddot{\hat{x}} + \dot{\hat{x}} = -\hat{U}'(\hat{x}) + a\cos(\omega\hat{t}) + f + \sqrt{2D}\hat{\xi}(\hat{t}), \quad (4)$$

where $\hat{x} = x/L$, $\hat{t} = t/\tau_0$, and $\tau_0 = \Gamma L^2/\Delta U$. The dimensionless mass $m$ is given by the ratio of two characteristic timescales, reading

$$m = \frac{\tau_1}{\tau_0} = \frac{M\Delta U}{\Gamma^2 L^2}, \quad (5)$$

where $\tau_1 = M/\Gamma$. We here emphasize the fact that the dimensionless mass $m$ depends not only on the actual physical mass of the particle $M$ but also on the friction coefficient $\Gamma$ as well as the parameters of the potential, i.e., on half of its barrier height $\Delta U$ and the period $L$. The strength of friction $\Gamma$ enters inversely the scaled mass value and it implies that the rescaled mass assumes in the regime of viscous moderate-large friction (i.e., operating at low Reynolds numbers, being typical for microsized particles immersed in solution [40,41]) a rather small value. The dimensionless noise intensity reads $D = k_B T/\Delta U$. The remaining quantities are explicitly defined as detailed in Ref. [35]. From here on, we stick throughout to these dimensionless variables. In order to simplify the notation, we will also omit the *hat* notation in Eq. (4).

The observable of main interest for mass separation is the directed velocity $\langle v\rangle$ of the particle, reading [35]

$$\langle v\rangle = \lim_{t\to\infty}\frac{1}{t}\int_0^t ds\langle\dot{x}(s)\rangle, \quad (6)$$

where $\langle\cdot\rangle$ indicates averaging over the thermal noise realizations as well as over the initial conditions for the position $x(0)$ and velocity $\dot{x}(0)$ of the Brownian particle. The latter is required in the deterministic limit $D \propto T \to 0$ when the dynamics may turn out to be nonergodic and dependent on specific choice of these initial conditions [42].

Knowingly, the Fokker-Planck equation corresponding to the Langevin Eq. (4) cannot be solved analytically in closed form. The task is thus to systematically analyze by comprehensive numerical means the emerging and rich variety of possible transport behaviors. The setup comprises a complex five-dimensional parameter space $\{m, a, \omega, f, D\}$. We nonetheless succeeded in performing the numerical analysis with unprecedented resolution. Overall, we considered nearly $10^9$ different parameter sets. The high precision was made possible solely due to an innovative computational method which is based on employing GPU supercomputers, for details see in Ref. [43].

The underlying symmetries of the Langevin dynamics in Eq. (4) imply that the directed velocity $\langle v\rangle$ behaves odd as a function of the external static bias $f$, i.e., $\langle v\rangle(-f) = -\langle v\rangle(f)$ so that $\langle v\rangle(f = 0) \equiv 0$ [3]. Generally, $\langle v\rangle$ is an increasing function in the direction of the static bias $f$ as one commonly would expect. The resulting particle transport velocity thus follows in the direction of the acting bias $f$, $\langle v\rangle = \mu(f)f$, with a positive-valued nonlinear mobility $\mu(f) > 0$. However, in the parameter space there occur also regimes for which the particle moves on average in the opposite direction to the applied bias; i.e., $\langle v\rangle < 0$ for $f > 0$ thus exhibiting anomalous transport in the form of NM with $\mu(f) < 0$ [26–29]. The key prerequisite for the occurrence of the latter phenomenon is that the system (i) is driven far from thermal equilibrium into a time-dependent *nonequilibrium* state, whose inertial dynamics does exhibit (ii) zero crossings of $\langle v\rangle$ [26,27]. In our case this condition is induced by the presence of the external time-periodic driving $a\cos(\omega t)$ which in turn *overrides* the limiting response behavior encoded with the Le Chatélier–Braun equilibrium principle [44], stating that at finite $f$ the response occurs into the

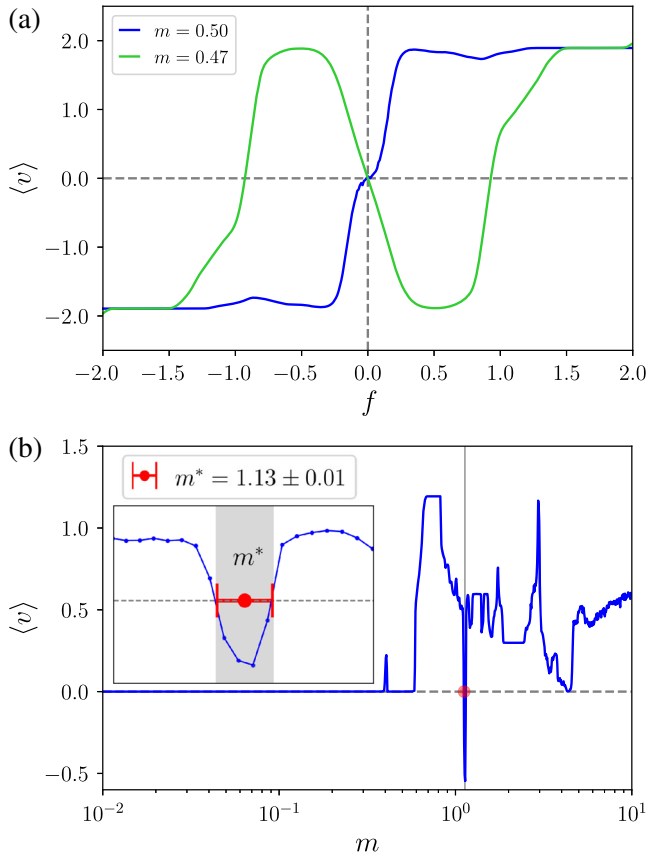


FIG. 1. (a) The force-directed velocity curve $\langle v \rangle(f)$ is depicted for the two parameter regimes corresponding to normal (blue) and anomalous (green) transport behavior in the form of NM. Note the sensitivity of the latter effect with respect to changes of the dimensionless mass $m$. The chosen parameters are $a = 10$, $\omega = 5.95$, and $D = 0.001$. (b) The directed velocity $\langle v \rangle$ versus mass $m$. In the inset we present the blow up (red region) showing the interval of the NM phenomenon as marked by the gray area. Parameters are $a = 5.125$, $\omega = 3.75$, $f = 1$, $D = 0.0001$.

direction of the applied force towards a new, displaced equilibrium.

With panel (a) of Fig. 1 we exemplify two force-velocity characteristics, $\langle v \rangle(f)$, corresponding to normal and NM transport behavior. Please note the sensitivity of the latter effect with respect to minute changes in the dimensionless mass $m$. A tiny change in mass by $\Delta m = 0.03$ is accompanied with the reverse of the particle response (note the blue line versus the green line behavior). There is seemingly no clear relationship detectable among the set of parameter values and the occurrence of this NM phenomenon. A small displacement in the parameter space may either cause a sudden emergence of NM or its rapid absence. One important observation is that typically it occurs in regimes for which the values of the parameters are *a priori* unknown. The interested reader is referred to the animation of the maps $\langle v \rangle(\omega, m)$ for several different magnitudes of the ac-driving amplitude $a$ which can be inspected on the web [45].

Among the regimes of NM in the parameter space there are tailored ones for which the latter phenomenon appears only for a very narrow interval of the mass $m$. This is illustrated with panel (b) of Fig. 1 where we depict the directed velocity $\langle v \rangle$ of the Brownian particle versus the mass $m$. An interesting transport property can be detected: among many particles with masses from a wide interval $m \in [10^{-2}, 10^{1}]$ only those with a mass $m \approx 1.13$ will move in the opposite direction $\langle v \rangle < 0$ to the acting bias $f = 1$. All other particles with positive velocity $\langle v \rangle$ will follow towards the direction of the bias. As a result, the particles with mass very close to $m \approx 1.13$ will be separated from all the others. This process of mechanical separation seems to be very promising provided that one would be able to control the mass $m^*$ of particles which are intended to be separated. The half-width $\delta m \approx 0.01$ of the interval where the NM occurs is indicated in the inset of the panel (b). It can be viewed as the resolution capacity for separation. However, we stress that typically NM in these intervals is sharply peaked, meaning that due to the clear difference between the magnitude of the negative velocity indeed only the particles with the precisely defined mass $m^*$ will be pronouncedly isolated from the others moving in the same or the opposite direction. We in turn undertook the attempt to search for such parameter regimes of the Langevin equation (4) that would enable us to control the occurrence of the NM by tuning just one parameter.

After this comprehensive numerical analysis we identified practically all sets of parameters $\{a, \omega, f, D\}$ for which NM emerges only for a narrow interval of mass $[m^* - \delta m, m^* + \delta m]$. Among selected parameter regimes, we focused on those which reveal a specific functional dependence between the isolated mass $m^*$ and the

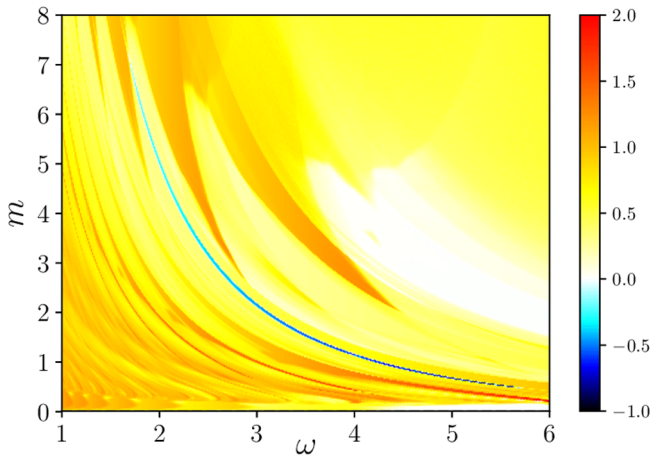


FIG. 2. Two-dimensional map of the directed velocity $\langle v \rangle$ of the Brownian particle as a function of the externally applied periodic driving frequency $\omega$ and mass $m$. The magnitude of velocity $\langle v \rangle$ is indicated by the color code with blue indicating regimes with NM. Chosen remaining parameters are set at $a = 5.9375$, $f = 1$, $D = 0.0001$.

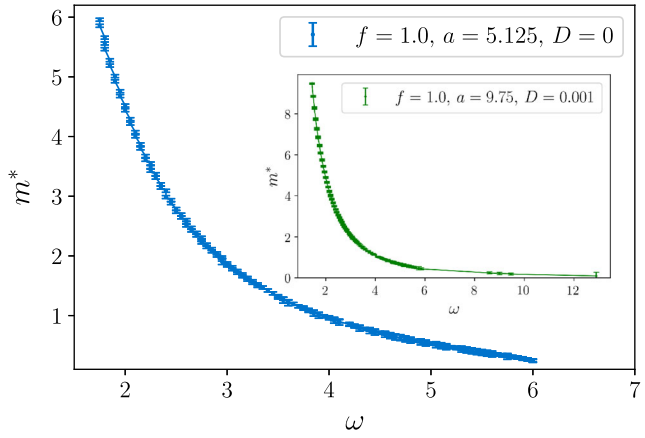


FIG. 3. The dependence of the mass $m^*$ tailored for separation as a function of the external driving frequency $\omega$ for zero temperature $D \propto T = 0$ with fixed $a = 5.125$ and $f = 1$. In the inset we present a different regime with $D = 0.001$ allowing for efficient and tunable mass separation via negative mobility.

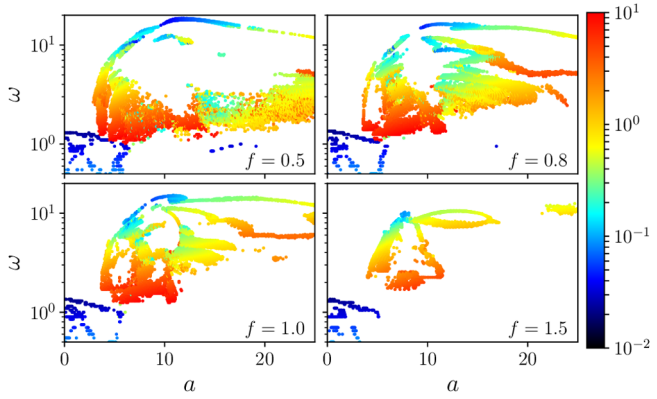


FIG. 4. The mass $m^*$ targeted for separation (color coded scale) via the NM effect as a function of the external ac-driving strength $a$ and frequency $\omega$ for different values of the bias $f$. Thermal noise intensity is set to zero $D = 0$.

parameter $a$, $\omega$, $f$, or $D$. In Fig. 2 we present such an example of the directed velocity $\langle v \rangle$ map as a function of the external driving frequency $\omega$ and scaled mass $m$. The magnitude of the velocity $\langle v \rangle$ is indicated with a corresponding color code. The blue regime corresponds to NM. It can be observed that for a given value of the frequency $\omega$ NM is present *solely* for a particular value of mass $m^*$. Therefore, using those tailored parameters read off from Fig. 2 we are able to tune the NM to the particle of a given mass $m^*$ by changing the value of the external driving frequency $\omega$ at fixed periodic driving strength. Doing so allows for efficient mass separation from an interval covering nearly 2 orders of magnitude.

In order to examine our results even more accurately we isolated the NM area from corresponding two parameter maps into a graph of the target mass $m^*$ versus the external driving frequency $\omega$. The result is depicted in Fig. 3 for zero temperature $D \propto T = 0$. A change of thermal noise intensity from $D = 0$ up to temperature $D \approx 0.0003$ does not significantly alter the desired characteristics which is quite robust with respect to temperature variation. Because NM derives from the complex deterministic dynamics, strong thermal noise of sufficient intensity is expected to cause a blurring of the phenomenon [35]. Interestingly, however, increasing thermal noise strength produces a shrinking of corresponding NM intervals, thereby optimizing the range $\delta m$. This feature implies an improvement of the selectivity for separation. In the inset of Fig. 3 we additionally depict different parameter regime allowing tunable mass separation for even higher temperature $D = 0.001$. Moreover, our method of mass separation is stable against a variation of the amplitude strength $a$ (not depicted). The effect is present for a wide range of amplitudes $a \in [4, 8]$. At this point we remark that the effect of mass separation upon harvesting the NM phenomenon is also present for the dependence $m^*(a)$ and alike for $m^*(f)$; the range of tunable mass separation proves, however, somewhat smaller.

Finally, we consider yet a further issue: Let us assume that we deal with a given mass $m^*$ which we want to separate from the rest. The question then is, for how many different masses $m^*$ taken from the extended interval $m^* \in [10^{-2}, 10^{1}]$ is it possible to isolate the sought-after parameter set $\{a, \omega, f, D\}$ for which only this very specific mass value $m^*$ displays NM, thereby allowing its separation in a most efficient unique manner. We note that for a single mass $m^*$ there might be several parameter regimes obeying this condition. The answer to this question is summarized with Fig. 4. There, the distribution of the mass $m^*$ targeted for separation via the NM phenomenon in the parameter plane of the ac-driving amplitude $a$ and frequency $\omega$ is depicted for different values of the static bias $f$. We observe that small masses can be isolated with low values of $a$ and $\omega$. Medium and large masses are separated when the amplitude and frequency assume moderate magnitudes. We detected that with this method and for a fixed bias value $f = 1$ nearly all masses from the considered interval can be isolated. We also find that the overall distribution of the mass $m^*$ targeted for separation depicted (in color) in Fig. 4 is robust with respect to a variation of bias $f$, noting that for smaller values of $f$ it undergoes a stretching.

In conclusion, this work provides an effective solution for the objective of the tunable mass separation. In our scheme, mass targeted for isolation can be controlled by nearly 2 orders of magnitude by merely changing the frequency $\omega$ of the external harmonic driving. This task apparently cannot be accomplished with similar quality by use of alternative methods such as filtration techniques or schemes which are based on fluid-driven Brownian motor methodology [1,46,47]. The approach presented here uses

only a spatially periodic nonlinear structure in combination with unbiased external time-periodic driving. Our method can further be adapted to the needs by proper fabrication of the nonlinear landscape described by its barrier height $\Delta U$ and period $L$. Other advantages are (i) as a representative of active techniques it offers an improved averaged migration speed as compared to alternative approaches [32], (ii) in contrast to microfluidic methods it allows the possibility to not only deflect different particle species along different transport angles, but even to steer them in opposite directions, (iii) use of small size of a lab-on-a-chip device technology together with advantageous fabrication costs allows for massive parallelization which makes high-throughput separation possible. We envision that the separation strategy proposed here provides mass selectivity required in present and future isolation of nano and micro particles, proteins, organelles and cells.

This work was supported by the Grants No. NCN 2017/26/D/ST2/00543 (J. S.) and No. NCN 2015/19/B/ST2/02856 (J. Ł.)

[1] P. Hänggi and F. Marchesoni, Rev. Mod. Phys. **81**, 387 (2009).
[2] P. Reimann, Phys. Rep. **361**, 57 (2002).
[3] S. Denisov, S. Flach, and P. Hänggi, Phys. Rep. **538**, 77 (2014).
[4] M. J. Skaug, Ch. Schwemmer, S. Fringes, C. D. Rawlings, and A. W. Knoll, Science **359**, 1505 (2018).
[5] Ch. Schwemmer, S. Fringes, U. Duerig, Y. K. Ryu Cho, and A. Knoll, Phys. Rev. Lett. **121**, 104102 (2018).
[6] M. Masaeli, E. Sollier, H. Amini, W. Mao, K. Camacho, N. Doshi, S. Mitragotri, A. Alexeev, and D. Di Carlo, Phys. Rev. X **2**, 031017 (2012).
[7] D. Reguera, A. Luque, P. S. Burada, G. Schmid, J. M. Rubi, and P. Hänggi, Phys. Rev. Lett. **108**, 020604 (2012).
[8] S. Meinhardt, J. Smiatek, R. Eichhorn, and F. Schmid, Phys. Rev. Lett. **108**, 214504 (2012).
[9] L. Bogunovic, M. Fliedner, R. Eichhorn, S. Wegener, J. Regtmeier, D. Anselmetti, and P. Reimann, Phys. Rev. Lett. **109**, 100603 (2012).
[10] P. Malgaretti, I. Pagonabarraga, and J. M. Rubi, Phys. Rev. Lett. **113**, 128301 (2014).
[11] S. Bo and R. Eichhorn, Phys. Rev. Lett. **119**, 060603 (2017).
[12] D. Matsunaga, F. Meng, A. Zöttl, R. Golestanian, and J. M. Yeomans, Phys. Rev. Lett. **119**, 198002 (2017).
[13] Q. Vagne and P. Sens, Phys. Rev. Lett. **120**, 058102 (2018).
[14] A. K. Mukhopadhyay, B. Liebchen, and P. Schmelcher, Phys. Rev. Lett. **120**, 218002 (2018).
[15] K. K. Zeming, S. Ranjan, and Y. Zhang, Nat. Commun. **4**, 1625 (2013).
[16] Z. Wang, A. Knebel, S. Grosjean, D. Wagner, S. Bräse, Ch. Wöll, J. Caro, and L. Heinke, Nat. Commun. **7**, 13872 (2016).
[17] G. Guan, L. Wu, A. A. Bhagat, Z. Li, P. C. Y. Chen, S. Chao, Ch. J. Ong, and J. Han, Sci. Rep. **3**, 1475 (2013).
[18] J. Zhang, S. Yan, R. Sluyter, W. Li, G. Alici, and N.-T. Nguyen, Sci. Rep. **4**, 4527 (2014).
[19] H. Jeon, Y. Kim, and G. Lim, Sci. Rep. **6**, 19911 (2016).
[20] Y. Li, H. Zhang, Y. Li, X. Li, J. Wu, S. Qian, and F. Li, Sci. Rep. **8**, 3618 (2018).
[21] S. Suresh, Acta Mater. **55**, 3989 (2007).
[22] B. Lindner, L. Schimansky-Geier, P. Reimann, P. Hänggi, and M. Nagaoka, Phys. Rev. E **59**, 1417 (1999).
[23] M. Borromeo and F. Marchesoni, Phys. Rev. Lett. **99**, 150605 (2007).
[24] P. Sajeesh and A. K. Sen, Microfluid. Nanofluid. **17**, 1 (2014).
[25] R. Eichhorn, P. Reimann, and P. Hänggi, Phys. Rev. Lett. **88**, 190601 (2002).
[26] Ł. Machura, M. Kostur, P. Talkner, J. Łuczka, and P. Hänggi, Phys. Rev. Lett. **98**, 040601 (2007).
[27] D. Speer, R. Eichhorn, and P. Reimann, Phys. Rev. E **76**, 051110 (2007).
[28] J. Spiechowicz, P. Hänggi, and J. Łuczka, Phys. Rev. E **90**, 032104 (2014).
[29] J. Nagel, D. Speer, T. Gaber, A. Sterck, R. Eichhorn, P. Reimann, K. Ilin, M. Siegel, D. Koelle, and R. Kleiner, Phys. Rev. Lett. **100**, 217001 (2008).
[30] A. Ros, R. Eichhorn, J. Regtmeier, T. T. Duong, P. Reimann, and D. Anselmetti, Nature (London) **436**, 928 (2005).
[31] R. Eichhorn, J. Regtmeier, D. Anselmetti, and P. Reimann, Soft Matter **6**, 1858 (2010).
[32] J. Luo, K. Muratore, E. Arriaga, and A. Ros, Anal. Chem. **88**, 5920 (2016).
[33] M. Schiavoni, L. Sanchez-Palencia, F. Renzoni, and G. Grynberg, Phys. Rev. Lett. **90**, 094101 (2003).
[34] E. Lutz and F. Renzoni, Nat. Phys. **9**, 615 (2013).
[35] A. Słapik, J. Łuczka, and J. Spiechowicz, Commun. Nonlinear Sci. Numer. Simul. **55**, 316 (2018).
[36] J. Spiechowicz and J. Łuczka, Sci. Rep. **7**, 16451 (2017).
[37] P. Reimann, C. Van den Broeck, H. Linke, P. Hänggi, J. M. Rubi, and A. Pérez-Madrid, Phys. Rev. Lett. **87**, 010602 (2001).
[38] B. Lindner and I. M. Sokolov, Phys. Rev. E **93**, 042106 (2016).
[39] J. Spiechowicz, P. Talkner, P. Hänggi, and J. Łuczka, New J. Phys. **18**, 123029 (2016).
[40] F. M. Purcell, Am. J. Phys. **45**, 3 (1977).
[41] E. Lauga, Soft Matter **7**, 3060 (2011).
[42] J. Spiechowicz, J. Łuczka, and P. Hänggi, Sci. Rep. **6**, 30948 (2016).
[43] J. Spiechowicz, M. Kostur, and Ł. Machura, Comput. Phys. Commun. **191**, 140 (2015).
[44] L. D. Landau and E. M. Lifshitz, *Statistical Physics, Part 1*, 3rd ed. (Pergamon Press, Oxford, 1980).
[45] https://github.com/jspiechowicz/mass-separation.
[46] C. Kettner, P. Reimann, P. Hänggi, and F. Müller, Phys. Rev. E **61**, 312 (2000).
[47] S. Matthias and F. Müller, Nature (London) **424**, 53 (2003).